Direct Observation of Nonaffine Tube Deformation in Strained Polymer Networks

W. Pyckhout-Hintzen, S. Westermann,* A. Wischnewski, M. Monkenbusch, and D. Richter
Jülich Centre for Neutron Science (JCNS1) and Institute for Complex Systems (ICS1), Forschungszentrum Jülich, D-52428 Jülich, Germany

E. Straube
FB Physik, University of Halle/Saale, D-06099 Halle, Germany

B. Farago and P. Lindner
Institute Laue-Langevin (ILL), F-38042 Grenoble Cedex 9, France
(Received 18 January 2013; published 10 May 2013)

We present a one-to-one comparison of polymer segmental fluctuations as measured by small angle neutron scattering in a network under deformation with those obtained by neutron spin echo spectroscopy. This allows an independent proof of the strain dependence of the chain entanglement length. The experimentally observed nonaffine square-root dependence of the tube channel on strain is in excellent agreement with theoretical predictions and permits us to exclude an often invoked nondeformed as well as affinely deformed tube.

DOI: 10.1103/PhysRevLett.110.196002 PACS numbers: 83.10.Kn, 81.05.Lg, 83.80.Va

The development of molecular-statistical theories for constitutive rubber laws witnessed a significant breakthrough with the concept of a mean field tube which accounts for topological chain-chain interactions. Tube concepts [1–4] were used for several decades to describe two principally similar but nevertheless intrinsically different systems. Entangled melts and rubberlike polymer networks are similar because for both systems at short times the topology is determined by the uncrossability of chains. They differ, however, in the fundamental aspect that the permanent cross-links of a network additionally freeze in the chain configurations and trap entanglements. This quenching of the tube blocks reptation or long time longitudinal motion along its profile in the network and limits the dynamics exclusively to local perpendicular motion. In the pioneering work by Deam and Edwards [5], the quenched disorder of such a randomly cross-linked network was successfully accounted for by introducing a harmonic restoring potential towards the mean configurations of the chains. Additional constraints due to the chain topology conservation were accounted for by appropriate contributions to this restoring potential [3,6]. Classical models of rubber elasticity fail in the consequent consideration of all constraints and mainly interpolate between both extremes of noninteracting phantom and fully affine theory.

For networks in which entanglement contributions still dominate the mechanical properties, the constraining potential was found to be anisotropic and governed naturally by the main axis directions of the deformation tensor [3]. The resulting fluctuation scale, which may be identified as the diameter of a confining tube, thereby showed a universal nonaffine and nontrivial square-root power law dependence on strain. This resulting molecular-statistical approach [3] performs well up to large deformations. The same under-affine strain dependence was reconfirmed from theory [7] and from experiment including multiaxial deformation [8]. The latter discredited approaches centered on restricted junction or chain fluctuations [9,10]. Very recently, the deformation dependence was revisited by Milner and co-workers from simulations of stretched rings [11]. There, the tube deforms, but to a lesser extent than the square-root law dictates. Furthermore, efforts to treat cross-linking and segmental fluctuations separately in a double network proved not particularly sensitive, either [12]. Experimentally, the length and strain dependence, on the other hand, were already probed successfully using small angle neutron scattering (SANS) on deformed networks, e.g., in [13].

Despite the important issue as to whether and how entanglements contribute to the stress-strain properties, a direct dynamic observation of the fluctuation range on a microscopic scale and thereby the ultimate proof of their strain dependence has been lacking to date. Such an experiment is all the more important since the extraction of fluctuation ranges from static SANS depended on the complex theoretical background which was applied to mechanical relaxation data and thus is in the same way indirect and biased. Direct access to the tube diameter by quasielastic scattering is therefore highly desirable.

In this work we therefore present the first comprehensive neutron spin echo (NSE) and SANS study on a deformed network. NSE experiments on long chain polymer melts are ideally suited to probe the segmental fluctuations in the relevant time and space intervals [14]. However, the challenge of inspecting deformed rubber with high resolution

neutron spectroscopy has not been realized before. Our results confirm both the size and the tube deformation dependence with $\sqrt{\lambda}$ if the strain is λ.

Monodisperse 1,4-polyisoprenes (PI) were anionically synthesized and characterized by membrane osmometry, light scattering, and size-exclusion chromatography. Basically symmetric hydrogenated (H) and deuterated (D) couples of PI were obtained (H: $M_w = 133$ kg/mol, $M_w/M_n = 1.02$; D: $M_w = 135$ kg/mol, $M_w/M_n = 1.02$). Randomly cross-linked networks were obtained for 50/50 H/D blends using dicumylperoxide as a cross-linker after solution blending and drying under high vacuum. The cross-linking was performed at 413 K and yielded a mesh size $M_c = (6700 \pm 500)$ g/mol between cross-links, determined from equilibrium swelling. The network chains thus carry on average 21 cross-links and 30 entanglement sections with molecular weight $M_e = 4500$ g/mol. Two strips of rubber were stretched simultaneously to a macroscopic strain $\lambda = (1.3 \pm 0.05)$ and glued in the stretched state on the inner sides of two quartz plates which were tightly sealed in a purified argon atmosphere. NSE experiments were performed in isotropic and stretched states at the IN11 spectrometer, ILL Grenoble, up to Fourier times of 40 ns at two scattering vectors $q = 0.121$ and 0.148 Å^{-1}. The samples were placed inside a nonmagnetic environmental chamber at 433 K under a flowing argon blanket. SANS experiments were performed under identical conditions on the D11 instrument, ILL Grenoble, covering the full scattering vector range $0.009 < q < 0.15$ Å^{-1} in the 2D detector plane. Additionally, a virgin isotropic network sample at room temperature was measured for reference. The 2D SANS data were corrected in the standard way pixelwise and absolutely calibrated with a 1 mm water standard. The isotropic network serves as the reference and was characterized by SANS [13]. From a 2D Debye fit the chain's radius of gyration in the untreated sample at RT yielded $R_g = (131.2 \pm 1)$ Å, which corresponds to a chain dimension ratio $R_g^2/M_w = (0.357 \pm 0.007)^2$ Å^2 mol/g for the used polyisoprene [13,15]. The isotropic NSE sample at elevated $T = 433$ K resulted in $R_g = (132.1 \pm 1)$ Å and agrees with an approximate chain expansion coefficient of about 10^{-4}/K. The SANS forward scattering intensity calculated from the sample composition is in very good agreement with the experimentally extrapolated level which confirms the absolute calibration of the network and the absence of isotope interactions. These observations thus provide the proper basis for an investigation of the strain dependence of the topology in the rubbers by scattering methods.

The anisotropic SANS data can be described in terms of a modified Warner-Edwards structure factor [6,13] with an effective tube from averaging over segment and cross-link fluctuations. There, d_0^{SANS}, the equilibrium tube diameter, is inserted *a priori* deformation dependent as obtained from free energy considerations in the Heinrich-Straube model [3] following $d_\mu = d_0^{\mathrm{SANS}}\sqrt{\lambda_\mu}$. In the 2D detector plane representation, the structure factor reads [3,6]

$$S(\vec{q},\lambda) = \int_0^1 d\eta \int_0^1 d\eta' \prod_\mu \exp\left(-(Q_\mu\lambda_\mu)^2(\eta-\eta') - Q_\mu^2(1-\lambda_\mu^2)\left\{\frac{d_\mu^2}{2\sqrt{6}R_g^2}\left[1-\exp\left(-\frac{(\eta-\eta')}{d_\mu^2/2\sqrt{6}R_g^2}\right)\right]\right\}\right). \quad (1)$$

Here, $Q_\mu = q_\mu R_g$, λ_μ is the microscopic strain along $\mu = x, y, z$ direction, and η, η' are the normalized contour length coordinates. Isotropic dangling ends of length f_e are accounted for by limiting the double integration to the tube-constrained section, $[f_e - (1 - f_e)]$ [16]. The well-known Debye function is retrieved for $\lambda = 1$ or $d_\mu \to \infty$. The anisotropy for a given λ is entirely determined by f_e and d_μ. Naturally, R_g is kept to the previously obtained isotropic value.

As cross-linking fully suppresses large scale translational diffusion and longitudinal segment motion, the quasielastic scattering is determined by displacements on the level of the mesh size of the fixed topology. This rubberlike behavior is treated appropriately within the Des Cloizeaux approach which is therefore perfectly suited for the interpretation of the NSE data [17,18]. This approach relieves the shortcomings of the de Gennes approach that is only applicable to melts [19] in which a longitudinal motion along the contour of the tube axis dominates, which is clearly incompatible with permanent networks.

The approach was originally formulated for an isotropic system in terms of one Cartesian coordinate to represent the system and its performance illustrated by a suitable comparison with published isotropic NSE data on an amorphous polyethylene melt [20]. It can, however, be easily generalized to fit the case under investigation here along the main axes of the deformation tensor of an anisotropic system simply by replacing $q^2 \to q_\mu^2$ and $x(\eta, t) \to x_\mu(\eta, t)$, where μ denotes a main axis direction and η is as previously defined. In this case, the mean square average spacing of the localized and fixed stress points, i.e., the main parameter of the approach, also transforms as $\langle S\rangle \to \langle S_\mu\rangle$. Its lengthy derivation is omitted and we only provide here a closed expression for $S(q,t)/S(q,0)$ in the limit for $t \to \infty$ representing the plateau levels in the dynamic structure factor solely determined by the tube size and the scattering vector,

$$\frac{S(q,\infty)}{S(q,0)} = \ln\left[1+\frac{q_\mu^2\langle S_\mu\rangle}{2}\right]\left(\frac{1}{q_\mu^2\langle S_\mu\rangle}+\frac{1}{q_\mu^2\langle S_\mu\rangle+2}\right). \quad (2)$$

On the same basis the static form factor was also derived [21]. The static comparison with stretched polystyrene data in SANS was already presented in the literature [22]. In our case, a description of NSE curves by this approach will immediately yield the requested length scales. The mean square fluctuations of a chain segment in the direction μ should then be given by

$$d_\mu^2 = 2\langle S_\mu \rangle / f, \tag{3}$$

where f is the functionality of the cross-link [23,24]. In this way, a strong similarity between the Warner-Edwards model and the Des Cloizeaux approach can be identified which justifies the comparison of fluctuation ranges and mean square distances. Since in our case $M_e \leq M_c$, i.e., the entanglement network is dominant, we assume $f = 2$ as for an uncross-linked chain. This leads then to the definition $d_\mu = \sqrt{\langle S_\mu \rangle}$ used by Des Cloizeaux himself. We note that consistently this definition underestimates the tube diameter in both static and quasielastic experiments by $\sim\sqrt{2}$ [18,20,22], but since we are not interested in the absolute agreement of the numerical value coming from different methods but merely on the strain dependence, the proper conclusions can still be drawn.

Figure 1 shows the normalized anisotropic 2D network SANS data $S(q_{\text{perp}}, q_{\text{para}})$ in the q range $0.01 < q < 0.12$ Å^{-1} at $T = 433$ K. This small-to-intermediate q range is sensitive to the tube diameter, and for this reason an overlap with the length scales accessed in the NSE experiment is given. Because of the relatively low deformation, the overall anisotropy of the SANS data is rather weak and a fit of d_0 and f_e is therefore not suitable. We therefore fixed the tube parameter to $d_0^{\text{SANS}} = 42$ Å, which we found consistently in similarly cross-linked rubbers for deformations up to even $\lambda = 3$ [13]. Refining then only the dangling end fraction, $f_e = (0.1 \pm 0.02)$ agrees well with the values expected from the cross-link density. The 2D representation in Fig. 1 is favored over the principal axes of deformation due to the rather poor sensitivity of the latter and the lack of consideration of important off-axis data.

In the subsequent Figs. 2 and 3 we present experimental data for the normalized intermediate structure factor $S(q, t)/S(q, 0)$ and the results of simultaneous fits from both scattering vectors which probe the tube length scale most sensitively since $qd_\mu \sim 1$. Compared to the isotropic state (Fig. 2), a clear deformation dependence for both q vectors can be noticed already. The reduced Rouse relaxation rate Wl^4, where W is the elementary Rouse rate and l is the statistical segment length, was obtained from the shortest times available in the isotropic experiment to be (26450 ± 1700) Å^4 ns^{-1} and was further fixed for the anisotropic evaluation. The monomeric friction coefficient ζ_0 in the network state, determined from $\zeta_0 = 3k_BTl^2/Wl^4$ yields, 3.5×10^{-12} Kg/s, which is virtually identical to the value on a PI melt, 3.8×10^{-12} kg/s, scaled to our temperature [20]. From this comparison we already conclude that the dynamics of segments is locally hardly influenced by the cross-links. A fit of the stress-point spacing $\sqrt{\langle S \rangle}$ in the isotropic network then yields the effective equilibrium tube diameter as $d_0 = (38 \pm 1)$ Å, which is only somewhat smaller than derived from anisotropic SANS measurements, i.e., 42 Å. The near-plateaus for each q value at the longest times measured are in good correspondence with the estimated amplitudes at $t \to \infty$ being 0.43 and 0.36, respectively, using Eq. (2).

The dynamic structure factors in the strained state already visually differ considerably from the quiescent network data and from each other in the height of the long time plateau and corresponding decay times. To allow comparison, the anisotropic NSE data were treated in the

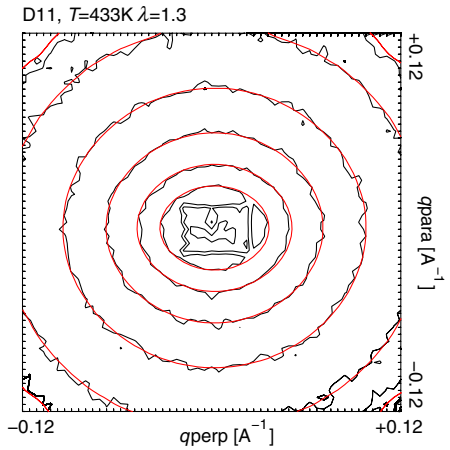

FIG. 1 (color online). $S(q_{\text{perp}}, q_{\text{para}})$ 2D SANS data for the q range between 0.01 and 0.12 Å^{-1}, i.e., $0.25 < qd < 3.5$. The strain direction was vertical. Solid gray (red) lines are obtained using the modified Warner-Edwards SANS model.

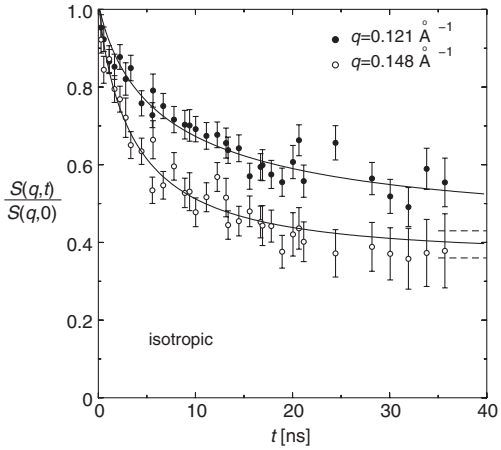

FIG. 2. $S(q, t)/S(q, 0)$ versus time at IN11 for the isotropic reference network sample. The tube size is $d_0 = 38$ Å from the Des Cloizeaux description at strain $\lambda = 1.0$ and $T = 433$ K. The dashed lines indicate the limit at $t = \infty$.

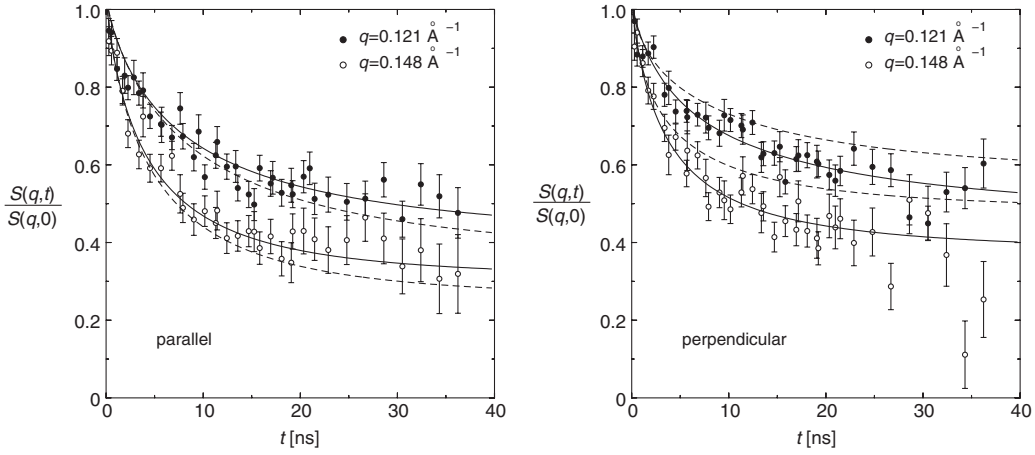

FIG. 3. Comparison of the measured and predicted dynamic structure factors $S(q,t)/S(q,0)$ for both directions parallel (left) and perpendicular (right) to the strain. Solid lines are the best fit with the Des Cloizeaux model whereas the dashed lines correspond to the affine predictions with the same model.

same way and the respective tube parameters were fitted for both q values simultaneously without constraints for both directions independently. In this way, the deformation dependence of the tube parameter is then a direct result of the modeling. Figure 3 summarizes the results: the solid lines correspond to the best fit of the Des Cloizeaux model for both directions. The respective tube parameters are $d_{\parallel} = (44.7 \pm 0.6)$ Å and $d_{\perp} = (37.4 \pm 0.5)$ Å. These directly measured values of d_{μ} agree within 1 Å with the expected values when one compares them to $d_{\parallel,\perp} = d_0\sqrt{\lambda_{\parallel,\perp}}$, which are 43.3 and 36 Å. On the contrary, model calculations with an affine deformation law $d_{\parallel,\perp} = d_0\lambda_{\parallel,\perp}$ are shown as dashed lines and clearly over- or underestimate the (q, t) dependence of the dynamic scattering function. The affine tube parameters would be 48 and 33 Å, respectively. This illustrates nicely the sensitivity of the quasielastic NSE method to ± 1 Å. $\lambda_{\parallel}$ and $\lambda_{\perp}$ are related to each other by the incompressibility assumption. Inversely, the experimental microscopic strain on the tube level obtained from $d_{\parallel}/d_{\perp} = \lambda^{3/4}$ and from the constant volume hypothesis is consistent with a microscopic chain deformation on the chain level $\lambda = (1.25 \pm 0.03)$. Within experimental error this is identical to the macroscopic sample deformation $\lambda = 1.3$, as can be expected for the underlying cross-link density of $\sim$20 kn per chain.

The measured effective localization range is a delicate average over both cross-link fluctuations and segmental exploration of the mean field entanglement tube. The first NSE experiment on a polymeric network under strain, providing direct access to the tube diameter in terms of the single chain dynamic structure factor, allowed us to unequivocally identify the coupling of chain fluctuations to the strain. This coupling follows the theoretically predicted square root dependence of the Heinrich-Straube and Panyukov-Rubinstein models. Based on the high sensitivity of NSE data on the tube diameter, a nondeformed or affinely deformed tube in a cross-linked polymer under strain can be ruled out. This dependence is essential in a constitutive material law which presently is rated as being of critical importance in engineering applications and in the continuum mechanics of rubber materials [8].

The authors thank T. Zinn for constructive discussions.

*Present address: Goodyear Innovation Center Luxembourg, Advanced Materials Science, Avenue Gordon Smith, L-7750 Colmar-Berg, Luxembourg.

[1] M. Doi and S. F. Edwards, *The Theory of Polymer Dynamics* (Oxford University Press, Oxford, England, 1986).
[2] P. G. De Gennes, J. Chem. Phys. **55**, 572 (1971).
[3] G. Heinrich, E. Straube, and G. Helmis, Adv. Polym. Sci. **85**, 33 (1988).
[4] T. C. B. McLeish, Adv. Phys. **51**, 1379 (2002).
[5] R. T. Deam and S. F. Edwards, Phil. Trans. R. Soc. A **280**, 317 (1976).
[6] M. Warner and S. F. Edwards, J. Phys. A **11**, 1649 (1978).
[7] M. Rubinstein and S. Panyukov, Macromolecules **30**, 8036 (1997).
[8] G. Marckmann and E. Verron, Rubber Chem. Technol. **79**, 835 (2006).
[9] P. Flory and B. Erman, Macromolecules **15**, 800 (1982).
[10] B. Erman and J. E. Mark, Macromolecules **20**, 2892 (1987).
[11] J. Qin, J. So, and S. T. Milner, Macromolecules **45**, 9816 (2012).
[12] B. Mergell and R. Everaers, Macromolecules **34**, 5675 (2001).
[13] S. Westermann, W. Pyckhout-Hintzen, D. Richter, E. Straube, S. Egelhaaf, and R. May, Macromolecules **34**, 2186 (2001).
[14] B. Ewen and D. Richter, Adv. Polym. Sci. **134**, 1 (1997).
[15] L. Ying, M. Kröger, and W. K. Liu, Polymer **52**, 5867 (2011).

[16] D. J. Read and T. C. B. McLeish, Macromolecules **30**, 6376 (1997).
[17] J. Des Cloizeaux, J. Phys. I (France) **3**, 1523 (1993).
[18] J. Wittmer, W. Paul, and K. Binder, J. Phys. II (France) **4**, 873 (1994).
[19] P. G. de Gennes, J. Phys. (Paris) **42**, 735 (1981).
[20] D. Richter, R. Butera, L. J. F. Fetters, J. S. Huang, B. Farago, and B. Ewen, Macromolecules **25**, 6156 (1992).
[21] J. Des Cloizeaux, J. Phys. I (France) **4**, 539 (1993).
[22] F. Boue, J. Bastide, M. Buzier, C. Collette, A. Lapp, and J. Herz, Prog. Colloid Polym. Sci. **75**, 152 (1987).
[23] H. M. James and E. Guth, J. Chem. Phys. **15**, 669 (1947).
[24] R. Ullman, Macromolecules **15**, 1395 (1982).